Journal of Constructional Steel Research 148 (2018) 450–456

Contents lists available at ScienceDirect

Journal of Constructional Steel Research

Fatigue performance and evaluation of welded joints in steel truss bridges

Chuang Cui [a], Qinghua Zhang [a,*], Yi Bao [b], Jiping Kang [a], Yizhi Bu [a]

[a] Department of Bridge Engineering, Southwest Jiaotong University, Chengdu, Sichuan 610031, China
[b] Department of Civil and Environmental Engineering, University of Michigan, 2350 Hayward St., Ann Arbor, MI 48109, USA

ARTICLE INFO

Article history:
Received 21 April 2018
Received in revised form 8 June 2018
Accepted 9 June 2018
Available online xxxx

Keywords:
Steel truss bridge
Fatigue resistance
Ultrasonic impact treatment
Corner-filleted profile
Fatigue evaluation

ABSTRACT

While welded joints are extensively used in the connections of steel truss bridges, service life of the bridges is largely dependent on the fatigue resistance of the welded joints. Stress concentration and weld residual stress are two primary causes of fatigue damage in the welded joints. In this study, corner-fillet profile (CFP) and ultrasonic impact treatment (UIT) are used to improve the fatigue performance of the welded joints through relieving stress concentration and weld residual stresses, respectively. The fatigue resistance of welded joints is evaluated through experimentation. The results indicate that the use of CFP and/or UIT can alter the initiation location of fatigue crack. The fatigue resistance of welded joints was increased by 24% and 36% by using the CFP and UIT, respectively. The fatigue performance of welded joints was evaluated using three different methods, including the nominal stress method, effective notch stress method, and peak stress method. The peak stress method with a single fatigue resistance curve demonstrated the highest applicability and accuracy.

1. Introduction

Steel trusses have been extensively used in railway bridges and hybrid highway-railway bridges. Steel truss bridges are typically constructed by assembling prefabricated truss components on site. Fig. 1 (a) and (b) show a representative cross section of a main girder in a hybrid highway-railway bridge. The girder is assembled using different truss components, including the chords, vertical posts, diagonal elements, etc. The components are connected through welding and/or using high-strength bolts. Integrated welded joints (Fig. 1(b)) are usually prefabricated in factory to ensure high welding quality. The welded joints between the flange and gusset plates are subjected to varying tensile stresses and other adverse effects on fatigue resistance, and thus susceptible to fatigue damages. In general, the adverse effects include stress concentration, weld defects and residual stresses at welded joints [1–4]. Under cyclic loading, cracks tend to initiate at the welded joints (Fig. 1(b)) and compromise the long-term durability of the truss bridge.

The effects of stress concentration, weld defect and residual stresses on fatigue resistance of welded joints have been investigated [1–9]. The stress concentration of steel truss joints has been studied through finite element analysis [1] and experimentation [2–9]. The geometry of weld joints was optimized, and a corner-filleted profile (CFP) at weld of cruciform joints was recommended to reduce stress concentration [5]. Effects of weld residual stresses on fatigue resistance of welded joints were evaluated [2]. The ultrasonic impact treatment (UIT), which is a metallurgical processing technique, was utilized to study the effects of residual stresses on fatigue resistance [6–8].

Different methods for evaluating fatigue resistance of welded joints have been proposed [10–12], with consideration of stress concentration and weld residual stress. Nominal stress method is recommended by several design specifications for steel structures, such as Eurocode 3 [10], IIW recommendation [11], AASHTO specifications [12], etc. Hot spot based methods have been applied to evaluate the fatigue performance of weld toe or weld root in different types of welded joints [3, 13–15]. Other methods with a single *S-N* curve have been presented for fatigue evaluation of specific weld details, such as the weld toe or weld root, including the effective notch stress method [16–19], and peak stress method [20–23]. The effective notch stress method was used to analyze the fatigue resistance of welded joints where fatigue cracks initiated at the weld toe or weld root using the maximum principal stress [16–19]. The peak stress method was developed based on the notch stress intensity and local strain energy [20–23]. The fillet welded joint is approximated as a V-shaped notch that has a notch-tip radius of zero. To date, there is still lack of research on using the effective notch stress method and peak stress method to investigate the fatigue resistance of welded joints and effect of CFP and UIT in steel truss structures.

This study aims to investigate the fatigue resistance of welded joints in steel truss bridges. To this end, 16 specimens were tested under cyclic loading. The effects of stress concentration and weld residual stress on fatigue resistance were considered in the experimental investigation.

* Corresponding author.
E-mail address: swjtuzqh@home.swjtu.edu.cn (Q. Zhang).

https://doi.org/10.1016/j.jcsr.2018.06.014
0143-974X/

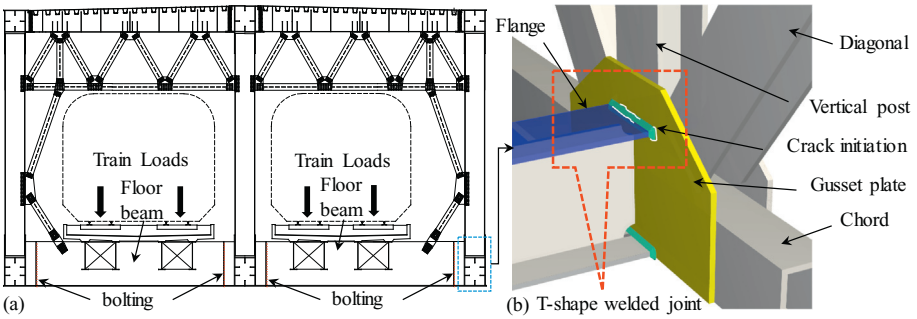

Fig. 1. Sketch of welded joint: (a) the cross-section; (b) the truss joint.

CFP and UIT were used to enhance the fatigue resistance of the welded joints. The nominal stress method, notch stress method and peak stress method are used to evaluate the fatigue resistance of the welded joints.

2. Experimental program

2.1. Specimens

Fatigue cracks often initiate at T-shape welded joints between the flange and the gusset plates, as shown in Fig. 1(b). To investigate the fatigue performance of T-shape welded joints, symmetrical cruciform welded specimens were used, as illustrated in Fig. 2(a) and (b). The two-pass gas metal arc welding is used in this study. The thicknesses of specimens were the same as those of the T-shape welded joints (Fig. 1(b)). CFP was employed to diminish the effect of the stress concentration, as shown in Fig. 2(a). For comparison, the corresponding specimen that does not have the CFP was used as control and tested to evaluate the effect of CFP on the fatigue resistance of the welded joints, as shown in Fig. 2(b).

To enhance the fatigue resistance of welded joints, UIT was applied to diminish the effect of the weld residual stress. In this study, the ultrasonic frequency was 20 kHz, and the impact frequency was 120 Hz. The indenter diameter was 4 mm, and oscillating amplitude of the output end of the waveguide was 50 μm. The output power, excitation voltage, and bias current were 250 W, 220 V, and 1.2 A, respectively. The dimensions of manual tool were 470 mm × 85 mm × 80 mm. The treatment speed in manual mode was 0.5 m/min. The treated workpiece region was weld toe. UIT was applied through repeating high-rate multi-directional impacts to the specimen surface in combination with ultrasonic vibration. This process was repeated for 4 times at each weld toe. The equipment and a sketch of the UIT operation are shown in Fig. 3.

To evaluate the effect of CFP and UIT on fatigue resistance of welded joints, three types of specimens were investigated: (1) specimens without CFP and UIT (designated as NCU), (2) specimens with CFP (designated as CFP), and (3) specimens with CFP and UIT (designated as CU). Each specimen was composed of three steel plates, two plates that simulate the flange (Fig. 1(b)) and one plate that simulates the gusset plate (Fig. 1(b)). The three plates were welded through metal inert gas welding, the same as that in real bridges.

The material of the test specimens is the hot-rolled low alloy steel Q370qD, which is a special structural steel for bridges. Two thicknesses of steel plates were used. Table 1 lists the mechanical properties and chemical composition of the steel Q370qD from mill certs.

2.2. Test setup and loading protocol

Fig. 4(a) shows the setup for cyclic tensile testing. Fig. 4(b) shows a specimen without CFP. Fig. 4(c) shows a weld joint of the specimen with CFP and UIT. Fatigue tests were conducted using a universal loading machine with a load capacity of 1500 kN. A total of 16 specimens were tested. The amplitude of the cyclic loading was constant for each specimen; different amplitudes and loading frequencies were applied to different specimens, as listed in Table 2. The lower bound of the cyclic load was set at 10 kN; the upper bound was changed to obtain the target load ranges. The effect of small change of load ratio on fatigue resistance was neglected [24, 25].

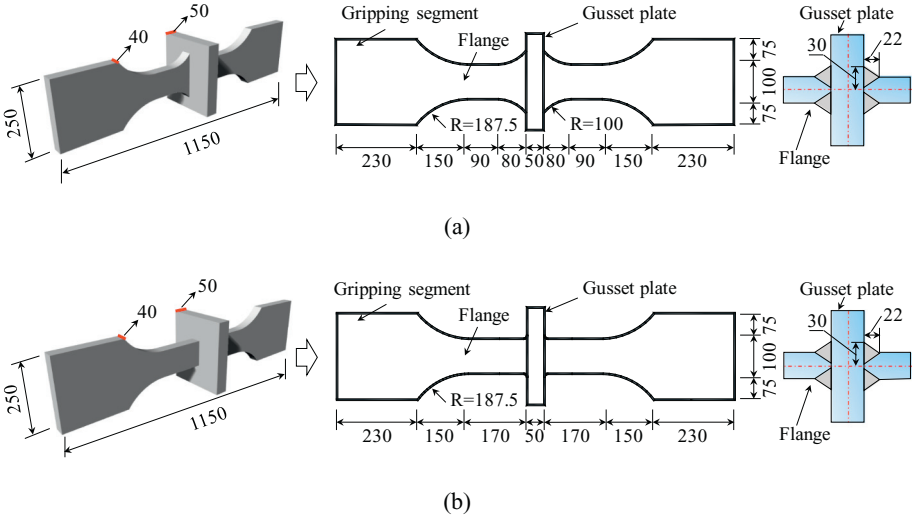

Fig. 2. Sketch of the specimens: (a) with CFP; (b) without CFP. (Unit: mm).

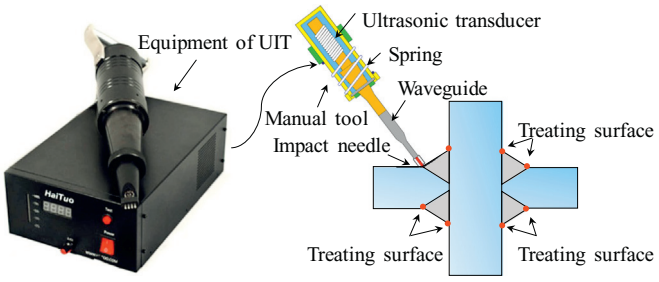

Fig. 3. Photograph of the equipment and sketch of UIT.

3. Experimental results and discussion

3.1. Testing results

The fatigue test results of the nominal stress range and failure cycle are listed in Table 3. The nominal stress represents the stress at the cross-section of cruciform connection surface in Fig. 2. To compare the fatigue resistance of different specimens, a fatigue resistance that is normalized to 2 million cycles is recommended in Eurocode 3 [10], as shown in Eq. (1).

$$\Delta\sigma_e = \left(\frac{n_f \Delta\sigma_n^3}{2\times 10^6}\right)^{1/3} \quad (1)$$

where $\Delta\sigma_e$is the equivalent fatigue resistance at 2 million cycles; $\Delta\sigma_n$ is the nominal stress ranges under external cyclic loading; n_f is the failure cycles.

It is noted that the failure cycle is the critical number of cycles when the specimens reach the ultimate capacity under cyclic nominal stress ranges. Therefore, the failure life includes the crack initiation and propagation. The equivalent fatigue resistance results (mean value ± standard deviation) of NCU, CFP and CU at 2 million cycles are 63.6 MPa ± 9.5 MPa, 83.7 MPa ± 11.8 MPa, and 101.6 MPa ± 12.5 MPa, respectively. The results demonstrate that the fatigue resistance of specimens without CFP and UIT is lower than the fatigue resistance of the specimens with CFP. Compared with the result of the specimens without UIT, the fatigue resistance of the specimens with UIT is much higher. Such comparison indicates that CFP and UIT are effective in enhancing fatigue resistance of the welded joints.

3.2. Failure analysis

The test specimens failed when the load capacity dropped below the applied load, due to initiation and propagation of fatigue cracks. In different specimens, fatigue cracks initiated at different locations, including the weld toe, weld root, and metal of flange plate. The failure patterns of specimens and typical fracture surfaces are illustrated in Fig. 5. The failure surface was a quarter ellipse or semi-ellipse.

Among the four NCU specimens, three specimens failed at the weld end of the flange plate edge, because of the higher level of the stress concentration at the flange plate edge, rather than the flange plate surface, as shown in Fig. 5(a); the other NCU specimen did not fail after it was loaded for >2 million cycles. Thus, the failures at the weld end of flange plate edge are dominant in the NCU specimens. All the six CFP specimens failed at the toe-root or root-toe near the flange plate surface (Fig. 5(b)), because of the lower level of the stress concentration at the flange plate edge with CFP. For the CU specimens, fatigue fracture occurred at the flange plate (base metal), due to enhanced fatigue resistance of cruciform welded joints (such as CU-2 and CU-5). Nevertheless, the fatigue fracture at weld root was dominant, because of the relaxation of residual stress at weld toe with UIT, as shown in Fig. 5(c).

4. Fatigue resistance evaluation

In this study, three methods are used to evaluate fatigue resistance of welded joints, including the nominal stress method, effective notch stress method, and peak stress method. The nominal stress is analyzed based on the fatigue test, while the other approaches are carried out by the numerical prediction techniques.

4.1. Nominal stress method

Based on the fatigue test results (Table 3), the fatigue resistance of the welded joints is determined using the nominal stress method, as shown in Figs. 6(a) to 6(c), where IIW 50, EC 63 and EC 80 respectively represent the nominal stress ranges of 50 MPa in IIW [11], 63 MPa in Eurocode 3 [10], and 80 MPa in Eurocode 3 at 2 million cycles. The fatigue resistance of NCU specimens is in accordance with IIW 50 (Fig. 6(a)); the fatigue resistance of CFP specimens is in agreement with EC 63; the fatigue resistance of CU specimens is in agreement with EC 80. Given the different *S-N* curves for the different geometry/weld residual stresses, the fatigue resistance of the welded joints can be evaluated using the obtained fatigue resistance curves.

Compared with the fatigue resistance of the welded joints without CFP, the fatigue resistance with CFP was improved by 26%. The fatigue resistance of the welded joints with UIT was increased by 34%. The fatigue resistance of the welded joints with both CFP and UIT was increased by 60%. It is revealed that CFP and UIT are efficacious to enhance the fatigue resistance of welded joints. Besides, by comparison of CFP and UIT, UIT is more effective than CFP to improve the fatigue resistance of welded joints. The arrows in Fig. 6 indicate that the specimens did not fail after they were loaded for the corresponding cycles.

4.2. Effective notch stress method

In comparison with the nominal stress method, the effective notch stress method considers the effect of local weld geometry at the fatigue critical points on the fatigue resistance of welded joints [18]. Stress concentration at the fatigue critical notch under the cyclic loading is analyzed using the effective notch stress method, based on the assumption of linear-elastic material behavior.

In this study, a three-dimensional solid element model was established using ABAQUS to analyze the fatigue resistance of welded joints. A rounded shape of the weld toe and root with a radius of 1 mm is used, following the IIW recommendation [11], was adopted in this study, as shown in Fig. 7(a) and (b).

The maximum principle stress at a notch represents the effective notch stress [26]. The effective notch stress in the NCU specimen at weld toe is larger than that of CFP or CU specimen, implying that the adverse effect of stress concentration on fatigue performance can be alleviated by the detail geometry with CFP. Besides, since the loaded

Table 1
Material and mechanical properties of Q370qD.

Thickness (mm)	Yield stress (MPa)	Ultimate tensile stress (MPa)	Elongation (%)	Chemical composition (wt%)					
				C	Mn	Si	S	P	Fe
50	385	535	30	0.15	1.43	0.35	0.006	0.017	98.05
40	395	645	26	0.13	1.46	0.28	0.003	0.014	98.11

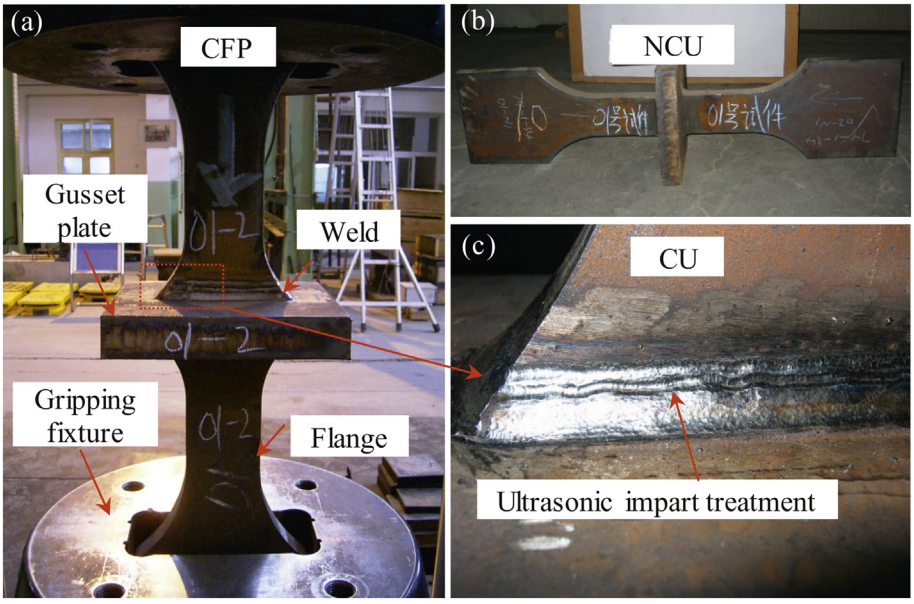

Fig. 4. The specimens of fatigue tests: (a) the loading of the specimen with CFP; (b) the specimen without CFP and UIT; (c) the photograph of ultrasonic impact treatment.

area of NCU specimen is less than that of CFP or CU specimen, the effective notch stress of NCU specimen at weld root is larger than that of CFP or CU specimen. According to Table 2, the effective notch stresses can be calculated through numerical simulations, assuming a linear-elastic material behavior.

To obtain the fatigue resistance curve that takes into consideration the effect of CFP and UIT, Eq. (2) is used to determine *S-N* curves through regression analysis of the fatigue test results.

$$\log N = \log C - m \log \Delta\sigma \tag{2}$$

where the C is a material constant; m is the inverse slope of the *S-N* curves. To determine the fatigue resistance in different cases, regression analyses of the fatigue resistance curve of welded joints were carried out under 50% and 97.7% possibility of survival, with a 95.5% confidence level. According to the specifications [10–12], m is taken as 3.

Fig. 8 shows four *S-N* curves. For the FAT225 curve, the fatigue resistance at 2 million cycles is 225 MPa. The other three *S-N* curves correspond to possibility of survival of 2.3%, 50%, and 97.7%, respectively. The lowest *S-N* curve ($\log N = 13.24 - 3 \times \log\Delta\sigma$) has a 97.7% possibility of survival; the fatigue resistance at 2 million cycles is 205 MPa, which is only slightly lower than the recommended value (225 MPa) in IIW [11]. Therefore, the curve is considered appropriate for fatigue resistance evaluation of the welded joints. It should be noted that the results in Fig. 8 are the effective notch stresses at the failure locations. After UIT was applied, fatigue failure did not occur at the weld toes of welded joints, indicating that the fatigue resistance of weld toes was enhanced by UIT. However, the fatigue resistance of weld toes was not quantified. In Fig. 8, $\Delta\sigma_{C,\,2.3\%}$, $\Delta\sigma_{C,\,50\%}$ and $\Delta\sigma_{C,\,97.7\%}$ respectively denote the effective notch stresses of the *S-N* curves that correspond to possibility of survival of 2.3%, 50%, and 97.7%, at $N = 2 \times 10^6$. A scatter index is introduced to quantify the level of scatter of the data points. The scatter index is defined as the ratio of $\Delta\sigma_{C,\,2.3\%}$, $\Delta\sigma_{C,\,97.7\%}$ at 2 million cycles. The scatter index of the effective notch stress method is 2.83 in this test.

Table 2
Applied cyclic loading of 16 specimens.

Designation	Loading (kN)		Loading frequency (Hz)	Designation	Loading (kN)		Loading frequency (Hz)
	Lower	Upper			Lower	Upper	
NCU-1	10	946	4.0	CFP-5	10	982	2.5
NCU-2	10	802	3.5	CFP-6	10	820	3.0
NCU-3	10	810	3.5	CU-1	10	1090	2.5
NCU-4	10	610	4.5	CU-2	10	802	3.5
CFP-1	10	1198	2.0	CU-3	10	730	3.5
CFP-2	10	712	3.5	CU-4	10	570	4.0
CFP-3	10	496	5.0	CU-5	10	890	3.5
CFP-4	10	1090	2.5	CU-6	10	1130	2.2

4.3. Peak stress method

Although fatigue resistance of the welded joints can be evaluated using the effective notch stress method, the large scatter index ($T = 2.83$) tends to compromise the accuracy of fatigue evaluation results of specimens with different geometrical details and weld residual stresses. For this reason, the peak stress method based on a notch-stress intensity factor is used to evaluate the fatigue resistance of welded joints [20]. The equivalent peak stress is determined using the ratio of notch-stress intensity factor to peak stress at the critical points of weld toe or root through finite element analysis. To obtain the

Table 3
List of fatigue test results.

Designation	Nominal stress range $\Delta\sigma_n$ (MPa)	Failure cycle	Fatigue resistance $\Delta\sigma_e$at 2 million cycles (MPa)	Failure locations
NCU-1	130	562,300	85.2	Weld toe
NCU-2	110	>2,034,000[a]	110.6	–[a]
NCU-3	111	212,600	52.6	Weld toe
NCU-4	83.5	516,700	53.2	Weld toe
CFP-1	220	94,000	79.4	Weld toe
CFP-2	130	950,400	101.4	Weld root
CFP-3	90	1,888,800	88.3	Weld root
CFP-4	200	72,600	66.2	Weld toe
CFP-5	180	140,800	74.3	Weld root
CFP-6	150	474,200	92.8	Weld toe
CU-1	200	280,500	103.9	Weld root
CU-2	146.7	918,428	113.2	Base metal
CU-3	133.3	413,900	78.9	Weld root
CU-4	103.7	>2,000,000[a]	103.7	–[a]
CU-5	163	662,200	112.7	Base metal
CU-6	207.4	218,700	99.2	Weld root

[a] The specimen did not fail after it was loaded with a certain number of loading cycles.

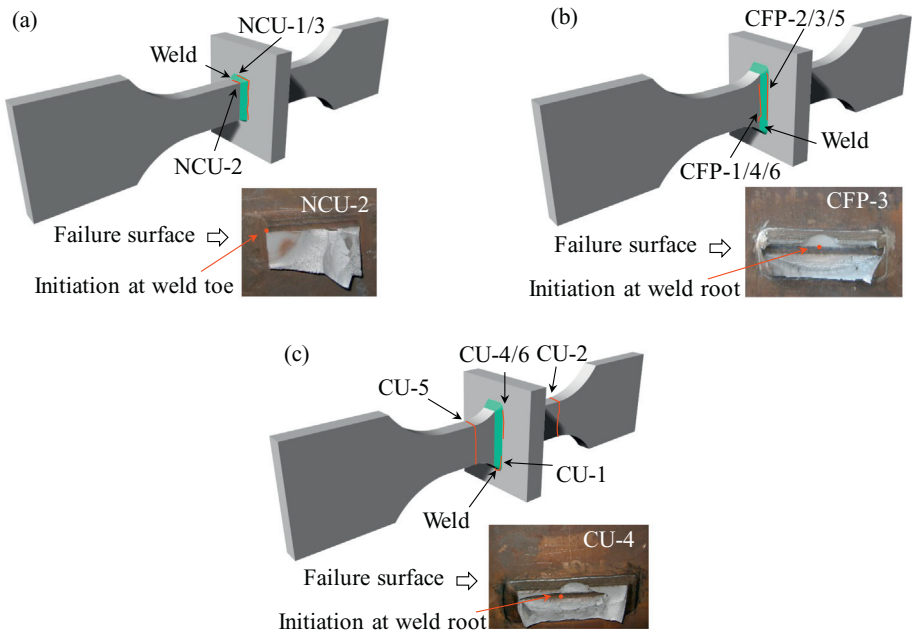

Fig. 5. Sketch of the failure modes and crack surfaces of the cruciform welded joints: (a) NCU specimen; (b) CFP specimen; (c) CU specimen.

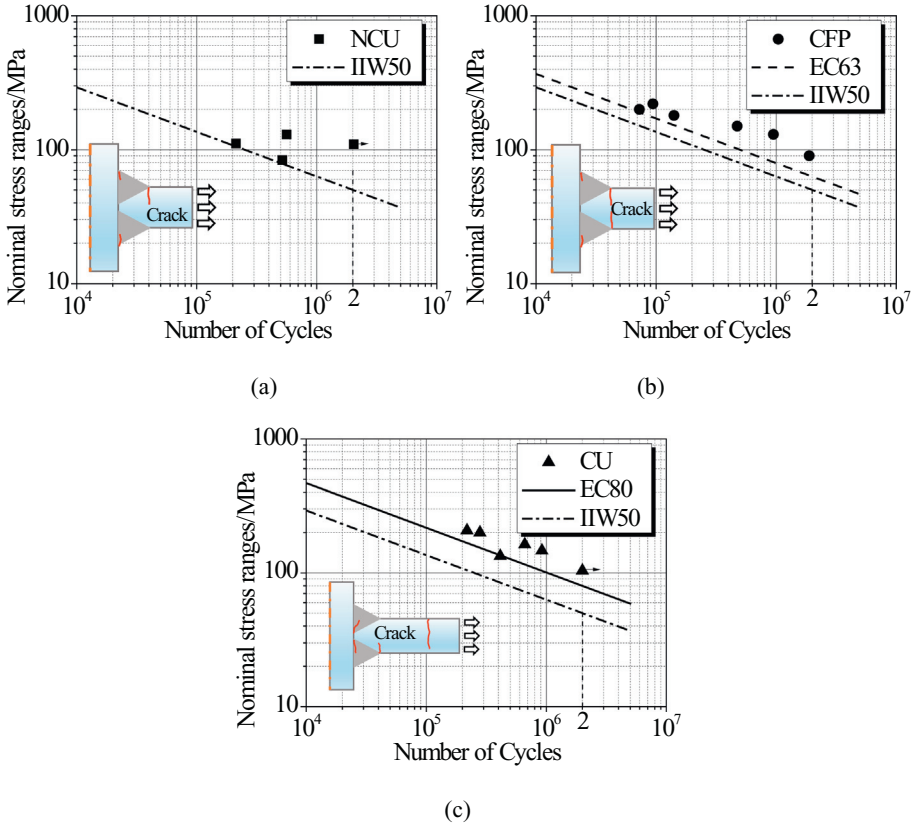

Fig. 6. Fatigue resistance evaluation by the nominal stress method at the welded joints: (a) NCU specimens; (b) CFP specimens; (c) CU specimens.

equivalent peak stress, the relationship between the strain energy density and stress intensity factor are determined using Eq. (3) [20–23]:

$$W = \frac{e_1}{E}\left[\frac{K_I}{R_0^{1-\lambda_1}}\right]^2 + \frac{e_2}{E}\left[\frac{K_{II}}{R_0^{1-\lambda_2}}\right]^2 \quad (3)$$

where W is the strain energy density; E is the Young's modulus; K_I and K_{II} are the stress intensity factors for Mode I and Mode II cracks, respectively; R_0 is the characteristic radius at the crack tip; λ_1 and λ_2 are the eigenvalues of the stress field for Mode I and Mode II cracks, respectively; e_1, e_2 are parameters depending on the notch opening angle 2α.

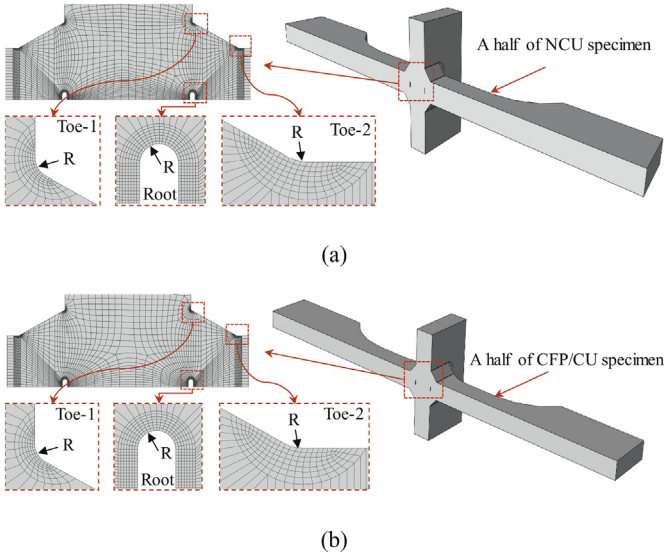

Fig. 7. Finite element model of notch stress ($R = 1$ mm): (a) NCU specimen; (b) CFP or CU specimen.

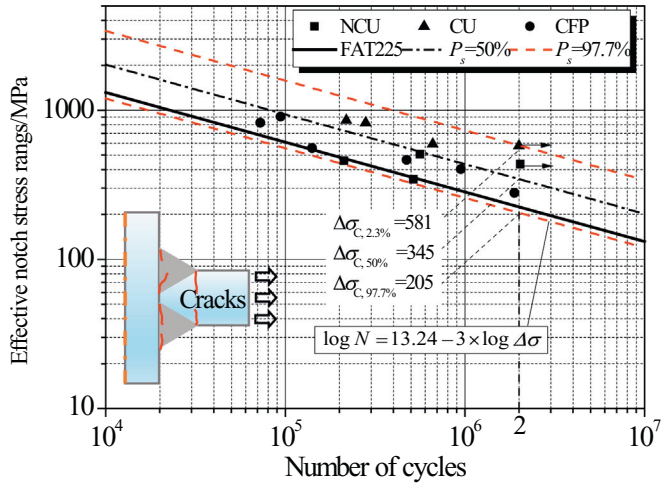

Fig. 8. Fatigue resistance evaluation by the effective notch stress method at the welded joints.

In cruciform welded joints, Mode I cracks are predominant [21–23], and thus Mode II cracks are neglected in this study. The strain energy density (W) can be expressed as.

$$W = \frac{e_1}{E}\left[\frac{K_I}{R_0^{1-\lambda_1}}\right]^2 \tag{4}$$

where, K_I can be determined using Eq. (5) [19–20].

$$K_{FE}^{*} = \frac{K_I}{\sigma_p d^{1-\lambda_1}} \cong 1.38 \tag{5}$$

where K_{FE}^{*} is the ratio of the notch stress intensity factor to peak stress (σ_p), and d represents the global mesh size in the finite element model. The value of K_{FE}^{*} is about 1.38 according to [22].

The peak stress at the critical points of the weld toe or root is the maximum principal stress. Under plane strain condition, the

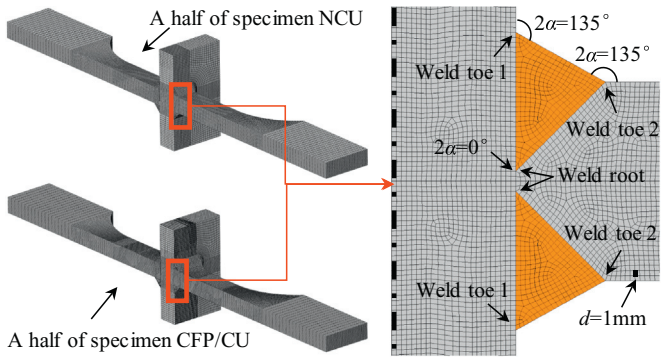

Fig. 9. Finite element model for peak stress method.

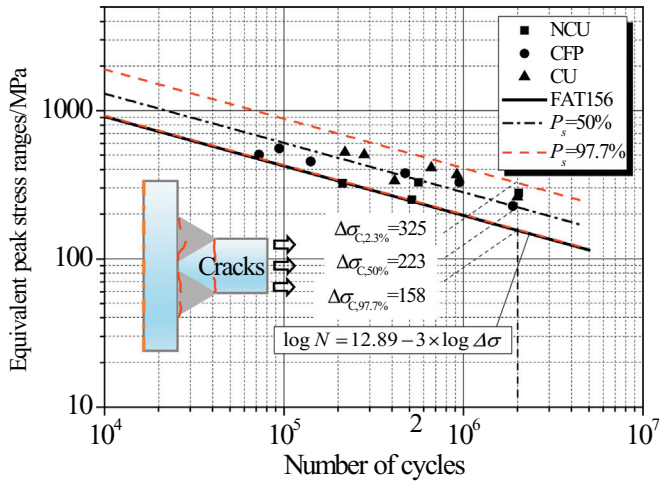

Fig. 10. Fatigue resistance evaluation by the peak stress method at the welded joints.

relationship between strain energy density and equivalent stress can be expressed in Eq. (6):

$$W = \frac{1-\nu^2}{E}\sigma_{eq}^2 \tag{6}$$

where σ_{eq} is the equivalent stress; ν is the Poisson's ratio.

Plugging Eq. (4) and Eq. (5) into Eq. (6), the relationship between the peak stress and the equivalent stress can be expressed in Eq. (7) [22].

$$\sigma_{eq} = 1.38\sqrt{\frac{2e_1}{1-\nu^2}}\left(\frac{d}{R_0}\right)^{1-\lambda_1}\sigma_p = f_w\sigma_p \tag{7}$$

where, $d = 1$ mm, $\nu = 0.3$ and $R_0 = 0.28$ mm, as recommended in [23].

Fig. 9 shows the finite element model established using ABAQUS. When $2\alpha = 0$, $e_1 = 133$, $\lambda_1 = 0.500$, $f_w = 1.410$; when $2\alpha = 135°$, $e_1 = 0.118$, $\lambda_1 = 0.674$, $f_w = 1.064$.

The equivalent stress ranges can be solved using the finite element analysis results and Eq. (5), as shown in Fig. 10. It is noted that the date points that correspond to crack initiation at flange plate are not included. "FAT156" means that the design fatigue resistance at 2 million cycles is 156 MPa [22]. The scatter index in the peak stress method equals to 2.05, which is much lower than 2.83 in the effective notch stress. It is demonstrated that the peak stress method has a higher prediction accuracy compared with the effective notch stress in the fatigue evaluation of welded joints. The lower-bound *S-N* curve ($\log N = 12.89 - 3 \times \log\Delta\sigma$) with a 97.7% possibility of survival below the mean *S-N* curve can be taken as the consistence fatigue resistance curve, where the fatigue resistance at 2 million cycles is 158 MPa, which is very

close to 156 MPa, as recommended in [22]. Compared with the effective notch stress method and nominal stress method, the peak stress method demonstrates a wider applicability and higher accuracy for fatigue evaluation of welded joints.

5. Conclusions

The main conclusions are summarized as follows:

(1) The use of CFP and/or UIT changed the fatigue failure mode of the welded joints. Fatigue cracks initiate at the flange plate edges for the welded joints without CFP, and on the flange plate surface for the welded joints with CFP. Fatigue cracks initiate at the weld root or weld of the welded joints with UIT, and at the weld toe of the welded joints without UIT.
(2) The use of CFP and UIT increased the fatigue resistance of welded joints by 24% and 36%, respectively. Combined use of CFP and UIT increased the fatigue resistance by 60%. Compared with CFP, the use of UIT was more effective in enhancing the fatigue resistance.
(3) The fatigue resistance of the welded joints at 2 million cycles was estimated 205 MPa and 158 MPa, using the effective notch stress method and peak stress method, respectively. The scatter index of the peak stress method was 2.05, which is much lower than 2.83 of the effective notch stress method, indicating that the peak stress method had a wider applicability and higher accuracy for fatigue evaluation of welded joints.

Acknowledgment

This research was Funded by the National Natural Science Foundation of China [grant numbers 51778533, 51578455, 50908192, and 51178394], Fundamental Research Funds for the Central Universities [grant number 2682014CX078], and National Science and Technology Support Program of China [grant number 2011BAG07B03], and Science and Technology Program of Hubei Transportation Department [grant number 2017-538-2-4].

References

[1] B. Cheng, Q. Qian, H. Sun, Steel truss bridges with welded box-section members and bowknot integral joints, part I: linear and non-linear analysis, J. Constr. Steel Res. 80 (2013) 465–474.
[2] C.M. Sonsino, Effect of residual stresses on the fatigue behaviour of welded joints depending on loading conditions and weld geometry, Int. J. Fatigue 31 (1) (2009) 88–101.
[3] Q. Zhang, C. Cui, Y. Bu, Y. Liu, H. Ye, Fatigue tests and fatigue assessment approaches for rib-to-diaphragm in steel orthotropic decks, J. Constr. Steel Res. 114 (2015) 110–118.
[4] X. Wei, L. Xiao, S. Pei, Fatigue assessment and stress analysis of cope-hole details in welded joints of steel truss bridge, Int. J. Fatigue 100 (2017) 136–147.
[5] A. Makris, T. Vandenbergh, C. Ramault, D. Van Hemelrijck, E. Lamkanfi, W. Van Paepegem, Shape optimisation of a biaxially loaded cruciform specimen, Polym. Test. 29 (2) (2010) 216–223.
[6] X. Cheng, J.W. Fisher, H.J. Prask, T. Gnäupel-Herold, B.T. Yen, S. Roy, Residual stress modification by post-weld treatment and its beneficial effect on fatigue strength of welded structures, Int. J. Fatigue 25 (9–11) (2003) 1259–1269.
[7] S. Roy, J.W. Fisher, B.T. Yen, Fatigue resistance of welded details enhanced by ultrasonic impact treatment (UIT), Int. J. Fatigue 25 (9–11) (2003) 1239–1247.
[8] H.C. Yildirim, G.B. Marquis, Fatigue strength improvement factors for high strength steel welded joints treated by high frequency mechanical impact, Int. J. Fatigue 44 (2012) 168–176.
[9] Q. Zhang, Y. Liu, Y. Bao, D. Jia, Y. Bu, Q. Li, Fatigue performance of orthotropic steel-concrete composite deck with large-size longitudinal U-shaped ribs, Eng. Struct. 150 (2017) 864–874.
[10] European Committee for Standardization (CEN), EN 1993-1-9, Eurocode3. Design of Steel Structures - Part 1–9: Fatigue. Brussels, 2005.
[11] IIW. Recommendations for fatigue design of welded joints and components. IIW-1823-07. , International Institute of Welding, 2008.
[12] American Association of State Highway and Transportation Offices. , AASHTO LRFD Bridge Design Specifications, Washington, DC, 2007.
[13] R. Liu, Y. Liu, B. Ji, M. Wang, Y. Tian, Hot spot stress analysis on rib–deck welded joint in orthotropic steel decks, J. Constr. Steel Res. 97 (2014) 1–9.
[14] P. Dong, A structural stress definition and numerical implementation for fatigue analysis of welded joints, Int. J. Fatigue 23 (10) (2001) 865–876.
[15] J.K. Hong, Evaluation of weld root failure using battelle structural stress method, J. Offshore Mech. Arctic Eng. 135 (2013) 420–431.
[16] M.R. Pradana, X. Qian, S. Swaddiwudhipong, Simplified effective notch stress calculation for non-overlapping circular hollow section K-joints, Mar. Struct. 55 (2017) 1–16.
[17] D. Radaj, C.M. Sonsino, W. Fricke, Recent developments in local concepts of fatigue assessment of welded joints, Int. J. Fatigue 31 (1) (2009) 2–11.
[18] W. Fricke, Guideline for the fatigue assessment by notch stress analysis for welded structures, The International Institute of Welding. IIW Doc. XIII-2240-08/XV-1289-08, 2008.
[19] M.R. Pradana, X. Qian, S. Swaddiwudhipong, W. Shen, An extrapolation method to determine the effective notch stress in circular hollow section X-joints, Fatigue Fract. Eng. Mater. Struct. 40 (2) (2017) 160–175.
[20] P. Livieri, P. Lazzarin, Fatigue strength of steel and aluminium welded joints based on generalised stress intensity factors and local strain energy values, Int. J. Fract. 133 (3) (2005) 247–276.
[21] P. Lazzarin, F. Berto, F.J. Gomez, M. Zappalorto, Some advantages derived from the use of the strain energy density over a control volume in fatigue strength assessments of welded joints, Int. J. Fatigue 30 (8) (2008) 1345–1357.
[22] G. Meneghetti, P. Lazzarin, The peak stress method for fatigue strength assessment of welded joints with weld toe or weld root failures, Welding in the World 55 (7–8) (2011) 22–29.
[23] P. Lazzarin, R. Zambardi, A finite-volume-energy based approach to predict the static and fatigue behavior of components with sharp V-shaped notches, Int. J. Fract. 112 (3) (2001) 275–298.
[24] O. Vosikovsky, The effect of stress ratio on fatigue crack growth rates in steels, Eng. Fract. Mech. 11 (3) (1979) 595–602.
[25] G.B. Marquis, E. Mikkola, H.C. Yildirim, Barsoum, Z. Fatigue strength improvement of steel structures by high-frequency mechanical impact: proposed fatigue assessment guidelines, Welding in the World 57 (6) (2013) 803–822.
[26] J. Heng, K. Zheng, C. Gou, Y. Zhang, Y. Bao, Fatigue performance of rib-to-deck joints in orthotropic steel decks with thickened edge U-ribs, J. Bridg. Eng. 22 (9) (2017), 04017059.